The co-modification of C_3N_4 by Pt single atom and cluster improves the photocatalytic hydrogen production performance

C. Q. Wu [a], G. H. Ni [a], X. Q Zhang [b], W. Yan [b,*]

[a] *School of Mechanical Engineering and Transportation, Changzhou Vocational Institute of Industry Technology, Changzhou, 213164, P. R. China*

[b] *School of Physics and Electronic Engineering, Jiangsu University, Zhenjiang, Jiangsu, 212013, P. R. China*

Photocatalytic hydrogen production is a kind of green hydrogen production technology. C_3N_4 semiconductor photocatalysis has attracted researchers' attention because of its non-toxic, harmless, and low-cost advantages. However, the low activity and carrier separation efficiency of the C_3N_4 photocatalyst are still unsatisfactory. In this study, the original C_3N_4 catalyst for H_2 production was improved by incorporating Pt single atoms and clusters as cocatalysts in a simple oil bath. The catalyst with the best activity, Pt/C_3N_4-7, exhibited a hydrogen production performance of 28.2 mmol/g/h, with an apparent quantum yield of 21.2% at a wavelength of 420 nm. It is 282 times and 3 times that of the original C_3N_4 and Pt nanoparticles-modified C_3N_4, respectively. The excellent electrical conductivity of Pt enhances the electron transfer between the triazine rings in C_3N_4 and the absorbance. Reducing carrier recombination and improving interlayer electron transfer significantly improve the photocatalytic hydrogen production activity.

(Received October 24, 2024; Accepted January 15, 2025)

Keywords: C_3N_4, Pt single atoms and cluster, Co-catalyst, Photocatalytic hydrogen production

1. Introduction

Human development in today's society cannot be separated from the consumption of fossil energy. Still, the use of fossil fuels will have an impact on the environment, such as CO_2 greenhouse gas, NO, and CO produced by incomplete combustion [1-3], and the amount is limited. This makes it imperative to find a sustainable and clean source of energy. H_2 has a high fuel value, and the product is pollution-free, considered the future replacement of fossil fuel energy [4-6]. Photocatalysis is much more economical and safe than the water gas and water electrolysis methods. Photocatalyst is an important part of the photocatalytic hydrogen process. Traditional catalysts for photocatalysis mainly include TiO_2, CdS, and C_3N_4 [7-10]. Among them, TiO_2 has a low utilization rate of light due to its large band gap width, while CdS is prone to photo corrosion, which reduces the photocatalytic activity [11-

* Corresponding author: yanwei_jsdx@163.com

https://doi.org/10.15251/DJNB.2025.201.55

15]. Carbon nitride (C_3N_4) has gained the favor of researchers due to its special two-dimensional structure and absence of metal components [16-17]. Although C_3N_4 is an organic semiconductor, C_3N_4 is physically and chemically stable. With the suitable conduction band position and small band gap width, C_3N_4 can absorb part of visible light, so that C_3N_4 can decompose in the water to produce hydrogen [18-20]. C_3N_4 photocatalytic hydrogen production also of problems with low activity and high carrier recombination efficiency [21]. In recent years, researchers have conducted many studies to solve this problem [22-25]. It is found that the supported co-catalyst is an effective method to inhibit carrier recombination because it can capture electrons and provide a highly active proton reduction site [26-27].

The precious platinum (Pt) is often valued as a highly effective cocatalyst for H_2 precipitation [28-30]. This is because Pt has a lower Femi level than C_3N_4, which facilitates capturing electrons (CB) from the conduction band [31-33]. Therefore, the addition of Pt to C_3N_4 has great potential to improve the photocatalytic H_2 evolution performance [34]. However, loading typical platinum nanoparticles leads to unsatisfactory utilization of platinum atoms. In recent years, single atoms catalysts have become a research hotspot. This is because reduced transition metal size can lead to more unsaturated coordination bonds and more active sites, thereby improving photocatalytic performance. Many experimental results have proved that single-atom catalysts can promote performance in various reactions [35-38]. For example, photocatalytic hydrogen production, CO oxidation, and other reactions showed good performance. Therefore, the Pt single atoms and cluster double cocatalysts are expected to further improve the photocatalytic performance.

In this experiment, we loaded Pt single atoms and clusters on the surface of C_3N_4 as co-catalysts and tested the hydrogen production performance of the sample under a 420 nm LED light source. The experimental results show that the H_2 generation performance of C_3N_4 modified with Pt single atoms and clusters could reach 28.2 mmol/g/h. Additionally, the H_2 production performance of C_3N_4 loaded with Pt nanoparticles by conventional photo deposition method is 9.8 mmol/g/h. The performance test showed that the H_2 generation performance of C_3N_4 modified by Pt single atoms and clusters was significantly improved, about 3 times and 282 times higher than that of Pt nanoparticles-modified C_3N_4 and pure C_3N_4.

2. Catalyst synthesis and characterization

2.1. Synthesis of C_3N_4

5 g urea was weighed and placed in an N_2 atmosphere. The heating rate of 2.5 ℃·min^{-1} was increased to 550 ℃ for a thermal reaction for 4 h, and C_3N_4 tablets were obtained when the furnace temperature dropped to room temperature.

2.2. Pt single atoms and nanoclusters co-modify C_3N_4

Weigh 50 mg C_3N_4 nanosheets were ultrasonically dispersed in 20 ml of water. Then 1 ml (2 g/l) of chloroplatinic acid was added, followed by a 70 ℃ oil bath for 3, 5, 7, 9, and 11 h. After filtration, samples were obtained by vacuum drying at 70 ℃. They are recorded as Pt/C_3N_4-3, Pt/C_3N_4-5, Pt/C_3N_4-7, Pt/C_3N_4-9 and Pt/C_3N_4-11. The synthesis process is shown in Fig. 1.

2.3. Photocatalytic hydrogen production test

Add 10 mg of the sample to 80 ml of 10% TEOA water solution. Then purge with Ar gas for 10 min. Then, the hydrogen content was measured by gas chromatograph (GC9720Plus, FULI INSTRUMENTS) every 1h under the irradiation of a 420 nm LED light source.

AQY calculation formula:

$$\mathrm{AQY} = \frac{amount\ of\ released\ hydrogen\ molecules\ in\ unit\ time \times 2}{number\ of\ incident\ photons\ in\ unit\ time} \times 100\%$$

2.4. Characterization techniques

The instrument used for X-ray diffraction (XRD) is Rigaku D/MAX-2500. The instrument used for HAADF-STEM is Rigaku JEM-ARM200F. The instrument used for X-ray photoelectron spectra (XPS) is Thermo Scientific K-Alpha. The instrument used for Ultraviolet-visible diffuse reflectance spectra (DRS) is UV2550, Shimadzu, Japan. The instrument used for Photoluminescence (PL) is JASCO FP-6500. Luminescence lifetimes were determined by a single photon counting spectrometer with an excitation source of 375 nm. The instrument used for Photocurrent response and Electrochemical impedance spectra (EIS) is CHI660B.

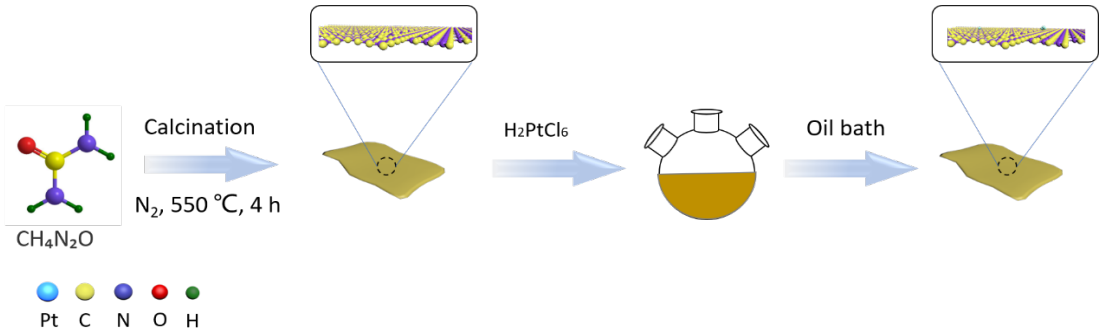

Fig. 1. Synthesis diagram of Pt/C_3N_4.

3. Results and discussion

3.1. Structure and morphology characterization

The X-ray diffraction (XRD) structure data of C_3N_4 are shown in Fig. 2a. In C_3N_4, the two characteristic peaks of 13° and 27° can be divided into (100) and (200) crystal faces [39], indicating the successful preparation of C_3N_4. There is no significant difference between the XRD of composite Pt/C_3N_4-7 and that of pure C_3N_4. In addition, no XRD peaks of Pt were observed in Pt/C_3N_4-7, indicating that the size of Pt is very small and may be single atoms or clusters. To further investigate the size of Pt, Pt/C_3N_4-7 was analyzed using TEM (Fig. 2b). The C_3N_4 was flaky, with no obvious granular Pt on it. The Pt size on Pt/C_3N_4-7 was analyzed by HADDF-TEM. As shown in Fig. 2c, bright spot single atoms and atomic clusters can be observed in the figure. The results show that we have successfully prepared Pt single atoms and Pt clusters on C_3N_4.

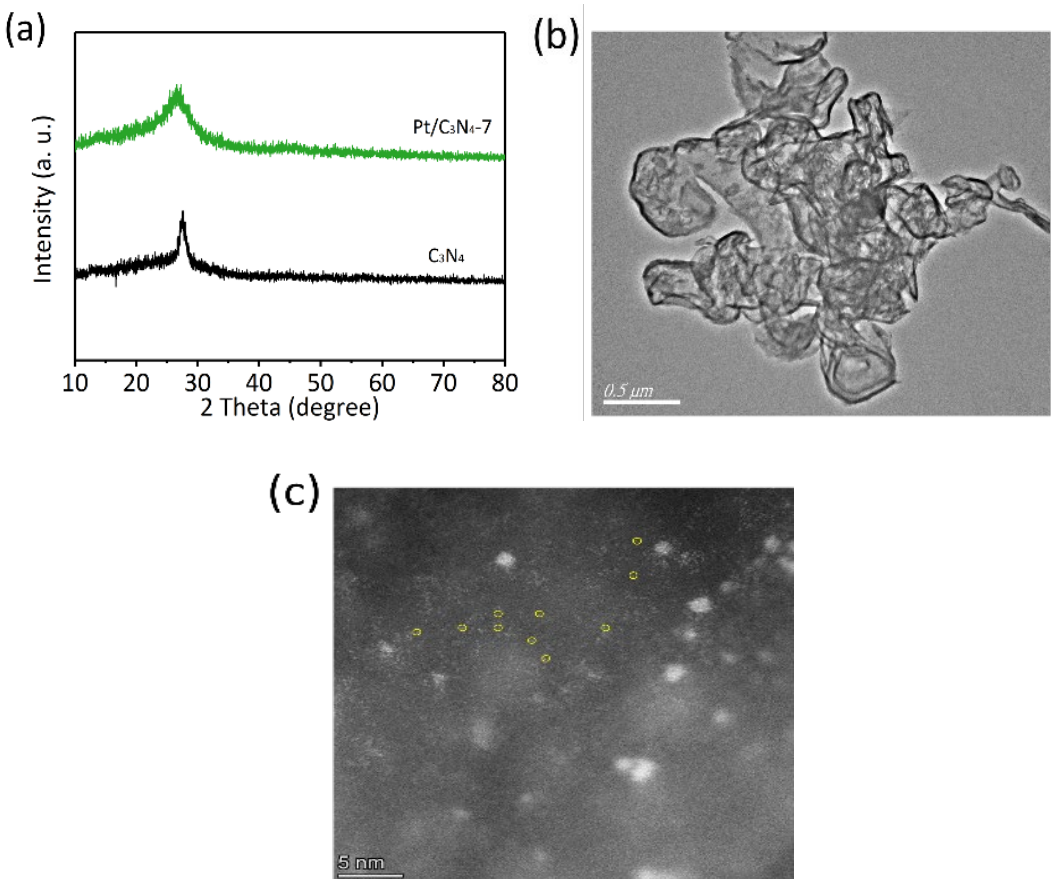

Fig. 2. (a) XRD of C_3N_4 and Pt/C_3N_4-7; (b) TEM and (c) HADDF-TEM of Pt/C_3N_4-7.

3.2. Performance analysis

The H_2 production and cycle stability of Pt/C_3N_4 with different reaction times were investigated. The experimental results depicted in Fig. 3a indicate that when utilizing C_3N_4-supported Pt as a cocatalyst, the H_2 production performance of the Pt/C_3N_4 composites attains a maximum value at a specific oil bath reaction time. The H_2 production performance of composite Pt/C_3N_4 was the best when the reaction time was 7 h. Fig. 3b shows the H_2 production rate of the sample. When the reaction time of the oil bath was 7 h, the best performance was 28.2 mmol/g/h, which is better than the 9.8 mmol/g/h of the Pt particle-modified C_3N_4 sample. Fig. 3c shows the quantum efficiency of Pt/C_3N_4-7 samples in different wavebands. Upon conducting tests, we found that the quantum efficiency of the composite Pt/C_3N_4-7 is 45.1% and 21.2% at 365 nm and 420 nm. Fig. 3d shows the stability test of photocatalytic H_2 production of composite sample Pt/C_3N_4-7. After 5 photocatalytic tests, the performance of Pt/C_3N_4-7 can still maintain a very high hydrogen production performance after 15 h of light without significant performance attenuation, which proves that the catalyst has extremely stable catalytic performance.

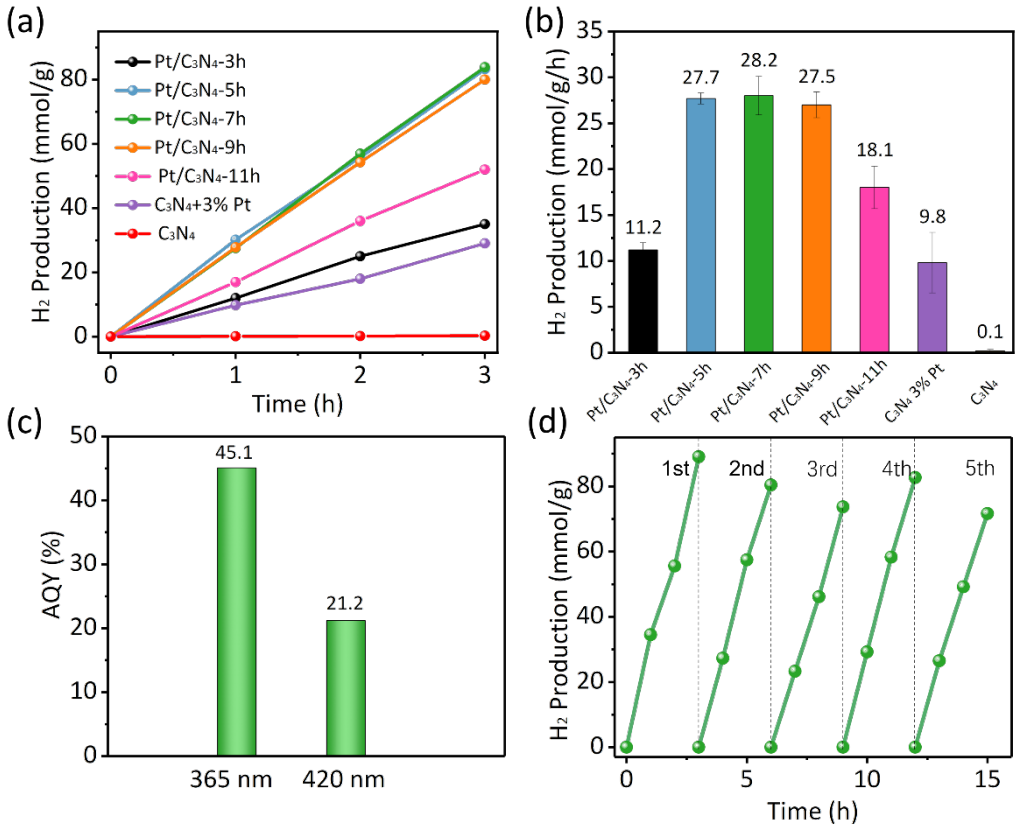

Fig. 3. (a) Hydrogen production diagram of different samples at 3 h (λ≥420 nm); (b) Hydrogen production of the as-obtained samples (λ≥420 nm); (c) AQY; (d) stability test of Pt/C_3N_4-7.

3.3. Chemical environmental and band structure analysis

The surface chemical environment of elements in the catalyst was detected by XPS photoelectron spectroscopy [40-41]. In Fig. 4a, three peaks can be observed from left to right in C 1s, which are C−C/C=C, C−NH_2, and (N−C=N) sp2 hybrid carbons in heterocycles, respectively [42]. In Fig. 4b, four peaks can be observed from left to right in N 1s, which are the signal of hybrid N in C−N=C, the N position of the three-element bridge, the presence of an unreacted amino group (C-NHx) at the edge of the tri-S-triazine ring, and the π-π excited state of the conjugated structure. In Fig. 4c, the peak corresponding to Pt^0 is observed at 75.2 eV and 72.1 eV. Meanwhile, located at 77.4 eV and 72.8 eV are Pt^{2+} [43].

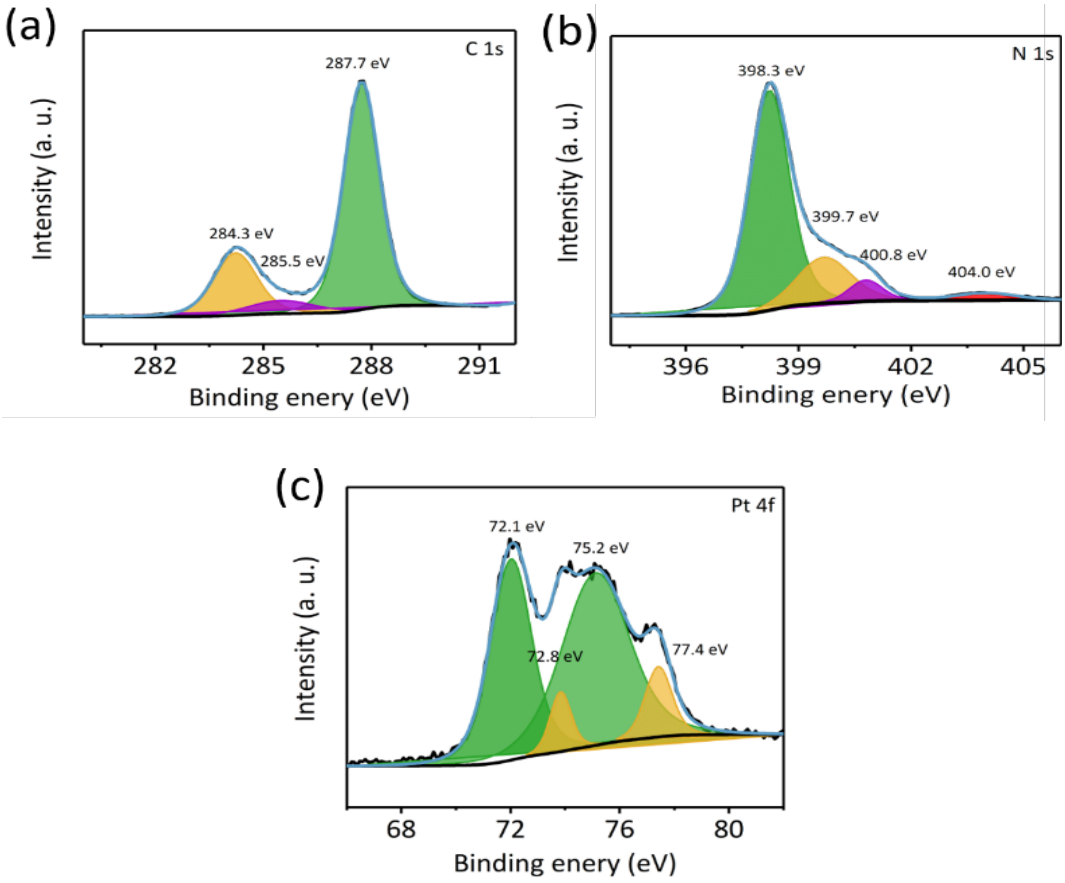

Fig. 4. (a) C 1s, (b) N 1s, and (c) Pt 4f of Pt/C_3N_4-7 high-resolution XPS spectrum.

DRS test can reflect the light absorption capacity of the samples [44-45]. DRS test results of pure C_3N_4 and Pt/C_3N_4-7 catalysts are shown in Fig. 5a. The addition of Pt enhances the light absorption of the material. Therefore, the bandgap widths of C_3N_4 and Pt/C_3N_4-7 catalysts can be calculated using the formula (1).

$$(\alpha hv)^{1/n} = A(hv - E_g) \quad (1)$$

The results are shown in Fig. 5b and 5c, the band gaps of C3N4 and Pt-C_3N_4-7 are 2.52 eV and 2.35 eV, respectively.

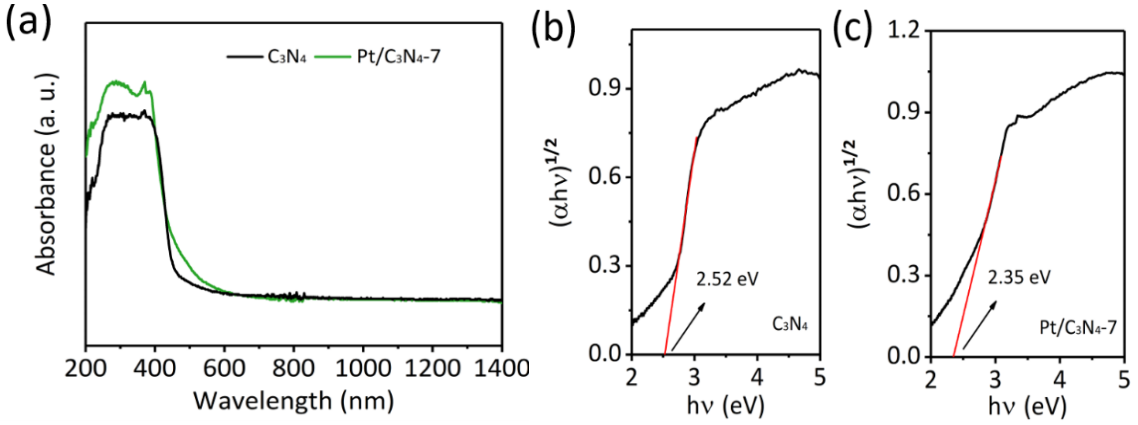

Fig. 5. Ultraviolet-visible diffuse reflection spectra (a) of samples; Kubelka-Munk transformed reflectance spectra (b) and(c) of C_3N_4 and Pt/C_3N_4-7.

3.4. Carrier separation efficiency analysis

The carrier separation efficiency can be analyzed by PL [46-47]. Fig. 6a displays the PL spectra of pure C_3N_4 and Pt/C_3N_4-7, where the excitation wavelength is 400 nm and the detection wavelength is 200 nm-800 nm. PL emission peak intensity of Pt/C_3N_4-7 is lower. This shows that the photogenerated carrier recombination rate of the Pt/C_3N_4-7 composite is low. This is mainly due to the improved photogenerated carrier separation after C_3N_4 loading Pt.

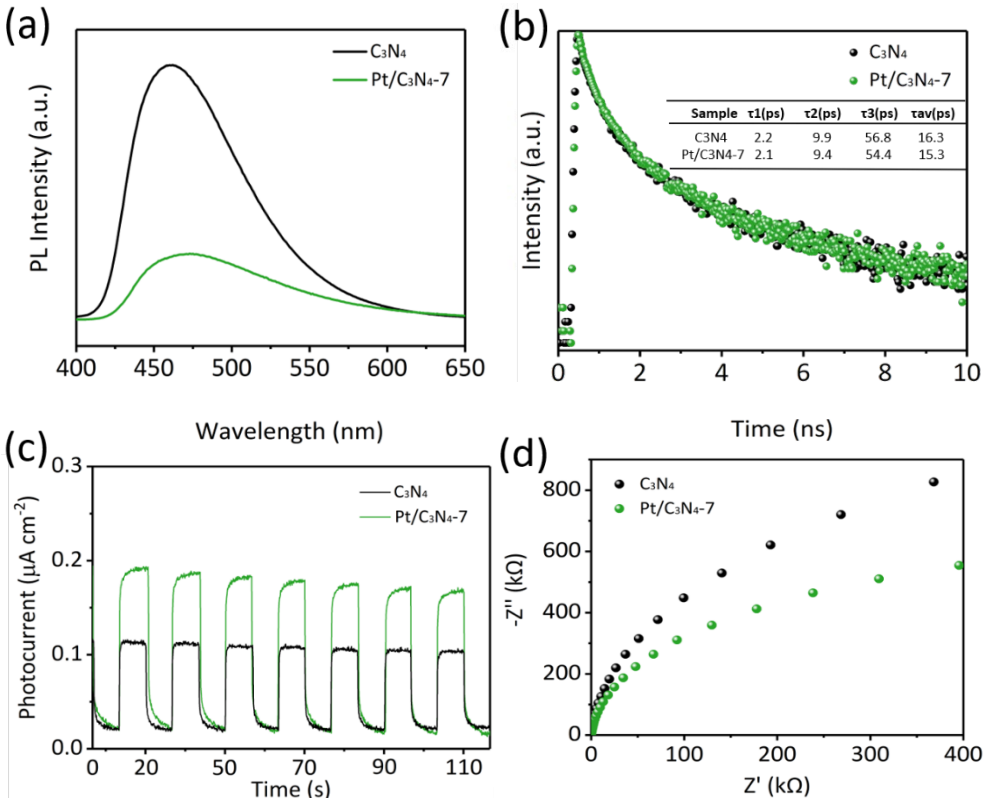

Fig. 6. PL and TRPL are (a) and (b) of C_3N_4 and Pt/C_3N_4-7, respectively; photocurrent responses and EIS Nyquist plots of C_3N_4 and Pt/C_3N_4-7 are (c) and (d) of C_3N_4 and Pt/C_3N_4-7, respectively.

The mean luminescent lifetime of Pt/C_3N_4-7 (15.3 ns) is shorter than that of pure C_3N_4, which means that the corresponding non-radiative decay caused by electron interactions will be increased, resulting in a shortened lifetime (Fig. 6b). To further verify the effective carrier separation in the semiconductor, transient photocurrent (i-t) and EIS tests were performed on the samples. As shown in Fig. 6c, the measured current density of Pt/C_3N_4-7 is higher, indicating that Pt/C_3N_4-7 can generate more photogenerated electrons and, consequently, exhibit greater photocurrent intensity under the same light source irradiation. In Fig. 6d, the radius of the EIS plot of Pt/C_3N_4-7 is smaller than that of C_3N_4. According to previous reports, the resistance increases with the increase of the radius, thereby proving that the relatively low resistance in the Pt/C_3N_4-7 sample is advantageous for the long-distance transport of photogenerated charges.

In light of the above discussion, the photocatalytic hydrogen production pathway of the Pt/C_3N_4-7 composite is illustrated in Fig. 7. C_3N_4 absorbs light and produces photogenerated electrons. Due to the strong electron affinity of Pt, photogenerated electrons produced by C_3N_4 will be transferred to two co-catalysts of Pt single atoms and Pt clusters. H^+ ions gain electrons from Pt single atoms and clusters, thereby producing H_2. The holes in C_3N_4 are consumed by the sacrificial agent TEOA.

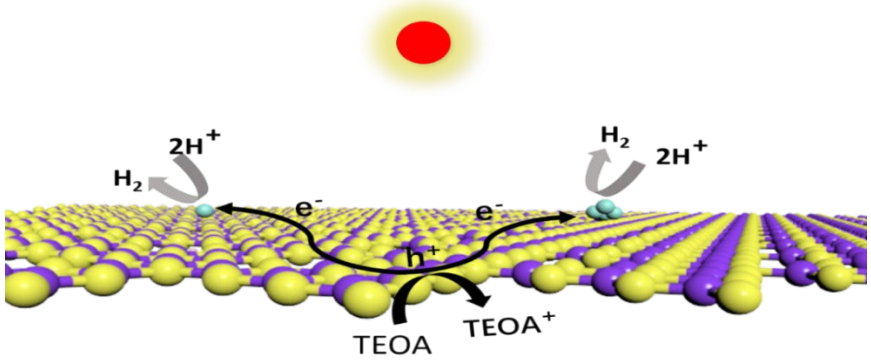

Fig. 7. Schematic diagram of Pt/C_3N_4-7 hydrogen production pathway.

4. Conclusion

In summary, we used the oil bath method to anchor Pt single atoms and clusters on C_3N_4. The photocatalytic hydrogen production yield of C_3N_4 modified by Pt single atom and cluster is much higher. The H_2 production rate of the sample with the optimal ratio of Pt/ C_3N_4 was 28.2 mmol/g/h. In comparison, the hydrogen production rate of the catalyst using the traditional photodeposition of Pt nanoparticles is 9.8 mmol/g/h. Results show that the performance of C_3N_4 modified by Pt single atoms and clusters is about 2.8 times that of C_3N_4 supported by Pt nanoparticles. Through fluorescence, electrochemical, and DRS tests, it has been proven that the Pt cocatalyst can effectively reduce the recombination of photo-generated electrons and improve light absorption of the sample. The Pt cocatalyst can effectively enhance the photocatalytic hydrogen production performance of C_3N_4.

Acknowledgments

This research was supported by the Industry-university-research cooperation project of Jiangsu Province (BA2019019)

References

[1] He P C, Zhou J, Zhou A W, et al., Chemical Journal of Chinese Universities-Chinese. 2019, 40(5): 855-866.

[2] Nakajima T, Tamaki Y, Ueno K, et al., Journal of the American Chemical Society. 2016, 138(42): 13818-13821; https://doi.org/10.1021/jacs.6b08824

[3] Lin JL, Li YF., Catalysis Science & Technology. 2020, 10(4): 959-966; https://doi.org/10.1039/C9CY02180A

[4] Ashtar M, Marwat MA, Yang Y, et al., International Journal of Hydrogen Energy. 2023, 48(84):32797-805; https://doi.org/10.1016/j.ijhydene.2023.05.084

[5] Xu Y, Xu J, Yan W, et al., Ceramics International. 2021, 47(7):8895-903; https://doi.org/10.1016/j.ceramint.2020.12.010

[6] Niu ZL, Yi SS, Li CQ, et al., Chemical Engineering Journal. 2020, 390:124602; https://doi.org/10.1016/j.cej.2020.124602

[7] Sopha H, Krbal M, Ng S, et al., Applied Materials Today. 2017, 9: 104-110; https://doi.org/10.1016/j.apmt.2017.06.002

[8] Zhao Q, Zhang B, Yao WF, et al., Catalysis Science & Technology. 2016, 6(24): 8474-8481; https://doi.org/10.1039/C6CY01896C

[9] Du ZY, Sun PJ, Wu KH, et al., Energy Technology. 2019, 7(7): 1900017; https://doi.org/10.1002/ente.201900017

[10] Cheng W, Ren X, Wang X, Huang Z, et al., Inorganic Chemistry. 2024, 63(30):14050-61; https://doi.org/10.1021/acs.inorgchem.4c01836

[11] Yue XZ, Li CQ, Liu ZY, et al., Applied Catalysis B: Environmental. 2019, 255:117760; https://doi.org/10.1016/j.apcatb.2019.117760

[12] Rawal SB, Kim HJ, Lee WI., Applied Catalysis B: Environmental. 2013, 142:458-64; https://doi.org/10.1016/j.apcatb.2013.05.067

[13] Li Y, Wang Z, Lv XJ., Journal of Materials Chemistry A. 2014, 2(37):15473-9; https://doi.org/10.1039/C4TA02890B

[14] Yan W, Xu Y, Hao S, et al., Inorganic Chemistry. 2022, 61(11):4725-34; https://doi.org/10.1021/acs.inorgchem.2c00045

[15] Wu X, Zhang H, Dong J, et al., Nano Energy. 2018, 45:109-17; https://doi.org/10.1016/j.nanoen.2017.12.039

[16] Idrees M, Amin B, Chen Y, et al., International Journal of Hydrogen Energy. 2024, 51:1217-28; https://doi.org/10.1016/j.ijhydene.2023.07.222

[17] Xu J, Zhang X, Chen X, et al., Inorganic Chemistry. 2024 Sep 11; https://doi.org/10.1021/acs.inorgchem.4c03268

[18] Xia P, Cao S, Zhu B, et al., Angewandte Chemie International Edition. 2020, 59(13):5218-25; https://doi.org/10.1002/anie.201916012

[19] He F, Zhu B, Cheng B, et al., Applied Catalysis B: Environmental. 2020, 272:119006; https://doi.org/10.1016/j.apcatb.2020.119006

[20] Fu J, Xu Q, Low J, et al., Applied Catalysis B: Environmental. 2019, 243:556-65; https://doi.org/10.1016/j.apcatb.2018.11.011

[21] Bi LL, Gao XP, Ma ZC, et al., Chemcatchem. 2017, 9(19): 3779-3785; https://doi.org/10.1002/cctc.201700640

[22] Chen Y, Su F, Xie H, et al., Chemical Engineering Journal. 2021, 404:126498; https://doi.org/10.1016/j.cej.2020.126498

[23] Xu F, Meng K, Cheng B, et al., Nature communications. 2020, 11(1):4613; https://doi.org/10.1038/s41467-020-18350-7

[24] Martin DJ, Qiu K, Shevlin SA, et al., Angewandte Chemie International Edition. 2014, 53(35):9240-5; https://doi.org/10.1002/anie.201403375

[25] Wang Y, Pham TN, Yan L, et al., Journal of Materials Chemistry C. 2022, 10(32):11791-800; https://doi.org/10.1039/D2TC02041F

[26] Li X, Zhao S, Duan X, et al., Applied Catalysis B: Environmental. 2021, 283:119660; https://doi.org/10.1016/j.apcatb.2020.119660

[27] Xu J, Zhang X, Yan W, et al., Inorganic Chemistry. 2024, 63(9):4279-87; https://doi.org/10.1021/acs.inorgchem.3c04408

[28] Zhou P, Lv F, Li N, et al., Nano energy. 2019, 56:127-37; https://doi.org/10.1016/j.nanoen.2018.11.033

[29] Chen Y, Ji S, Sun W, et al., Angewandte Chemie. 2020, 132(3):1311-7; https://doi.org/10.1002/ange.201912439

[30] Xu T, Zheng H, Zhang P., Journal of hazardous materials. 2020, 388:121746; https://doi.org/10.1016/j.jhazmat.2019.121746

[31] Zhu YQ, Wang T, Xu T, et al., Applied Surface Science. 2019, 464: 36-42; https://doi.org/10.1016/j.apsusc.2018.09.061

[32] Kumar S, Pandit V, Bhattacharyya K, et al., Materials Chemistry and Physics. 2018, 214: 364-376; https://doi.org/10.1016/j.matchemphys.2018.04.113

[33] Lin JJ, Sun T, Li MB, et al., Journal of Catalysis. 2019, 372: 8-18; https://doi.org/10.1016/j.jcat.2019.02.019

[34] Cao SW, Jiang J, Zhu BC, et al., Physical Chemistry Chemical Physics. 2016, 18(28): 19457-19463; https://doi.org/10.1039/C6CP02832B

[35] Yang Y, Zeng G, Huang D, et al., Small. 2020, 2001634; https://doi.org/10.1002/smll.202001634

[36] Ma M, Huang Z, Doronkin DE, et al., Applied Catalysis B: Environmental. 2022, 300:120695; https://doi.org/10.1016/j.apcatb.2021.120695

[37] Li Y, Li B, Zhang D, et al., ACS Nano. 2020, 14(8):10552-61; https://doi.org/10.1021/acsnano.0c04544

[38] Cao Y, Guo L, Dan M, et al., Nature communications. 2021, 12(1):1675;

https://doi.org/10.1038/s41467-021-21925-7

[39] Long D, Chen WL, Rao X, et al., Chemcatchem. 2020, 12(7): 2022-2031; https://doi.org/10.1002/cctc.201901958

[40] Liu M, Ye P, Wang M, et al., Journal of Environmental Chemical Engineering. 2022, 10(5):108436; https://doi.org/10.1016/j.jece.2022.108436

[41] Liu H, Li P, Qiu F, et al., Advanced Materials Interfaces. 2018, 5(19): 1800859; https://doi.org/10.1002/admi.201800859

[43] Ma JY, Tan XJ, Zhang QQ, et al., ACS Catalysis. 2021, 11(6): 3352-3360; https://doi.org/10.1021/acscatal.0c04943

[44] Xu J, Zhu S, Zhou H, et al., Catalysts. 2024, 14(6):356; https://doi.org/10.3390/catal14060356

[45] Xu J, Cheng W, Liang X, et al., Journal of Alloys and Compounds. 2024, 1003:175610; https://doi.org/10.1016/j.jallcom.2024.175610

[46] Liu S, Huang J, Su H, et al., Ceramics International. 2021, 47(1):1414-20; https://doi.org/10.1016/j.ceramint.2020.08.265

[47] Wang L, Hu Y, Xu J, et al., International Journal of Hydrogen Energy. 2023, 48(45):16987-99; https://doi.org/10.1016/j.ijhydene.2023.01.172